Surface Segregation of Boron in Dispersion-Strengthened Copper[*]

D. E. Gallagher, E. W. Hoyt and R. E. Kirby

Stanford Linear Accelerator Center,

Stanford University, Stanford, California 94309, USA

ABSTRACT

The improved yield strength of annealed dispersion- strengthened copper (DSC) over conventional OFE copper makes it a possible candidate for use in extremely high potential gradient particle accelerator structures where stability is of critical importance. Test brazes of such structures show that the surface of DSC is not readily wetted by conventional gold-based braze alloys used for copper. Surface analyses (by XPS and AES) of samples raised to brazing temperature show the presence of boron, which diffuses to the surface and possibly interferes with the wetting process. Boron is an intentional oxygen scavenger added to the DSC during manufacture. Alumina, the primary additive in the strengthening process, is not detected on the surface.

Keywords: Copper, accelerator, XPS

1. Introduction

Dispersion-strengthened copper (DSC) is a high mechanical strength, high thermal and electrical conductivity engineering alloy which is being investigated as an alternative to standard oxygen-free high-conductivity (OFE) copper in high energy physics applications where both these properties are desirable. It is of particular interest in the manufacture of structures required to function in high potential gradient environments, since it has been observed that surface hardness is among the factors affecting electrical breakdown voltage [1], and also in large structures for which OFE copper is unsuitably soft and deformable.

The material consists of a dispersion of less than one volume percent of alumina particles, on the order of 60–200 Å in size, throughout a matrix of pure copper, which may be made to an oxygen-free specification by the addition of a small amount of boron (typically 150 ppm by weight). The microstructure of copper that includes these alumina dispersoids is such that grain boundaries are kept short, and since it is along these that glide dislocations normally occur, the particles thereby inhibit such movement within the material, and make it harder. This high mechanical strength relative to OFE Cu is retained even after protracted exposure to high temperatures, because the dispersal of fine oxide particles acts to interrupt grain growth as well as dislocation movement, and the microstructure outlined above is therefore extremely stable. Thus the unannealed yield strength of DSC is 25% higher than that of cold-worked OFE material at room temperature, whereas the annealed strength of DSC is 13 times the corresponding value for the same full anneal of OFE [2]. The boron, without itself alloying with the copper, acts as an oxygen scavenger, and thus reduces reaction of the latter with hydrogen introduced in the manufacture of the alloy, which otherwise results in blister formation due to the large internal pressures of water vapor that can develop during subsequent brazing at high temperatures.

This particular investigation was begun following the observation that some batches of DSC being studied at SLAC, supplied under the tradename "Glidcop AL-15" [3], did not wet well during brazing with gold-based alloys at 1000°C, and that a sample of the same material (unbrazed) underwent a change during an experimental vacuum annealing in an

UHV rf furnace which left its surface contaminated by a faint whitish film. The purpose of this investigation was to identify the nature of this film and whether it might be connected to the brazing performance.

2. Experiments

2.1. *Specimen preparation*

Samples were prepared by machining Glidcop AL-15 material with sulfur-free water-based coolant, mechanically polished with diamond ($0.25\,\mu$ final particle size), and subsequently cleaned for ultra-high vacuum use. Three samples were analyzed in all: (a) One "control," analyzed following cleaning; (b) One heated to ca. 1000°C for several minutes in an UHV rf furnace attached to the surface spectrometer system, cooled to room temperature, analyzed in situ, exposed to room air, and re-analyzed; (c) One fired to 1025°C in a dry-H_2 brazing furnace, purged to atmosphere with N_2 during cooldown and inserted into the surface spectrometer system for analysis.

2.2. *Analytical instrumentation*

Surface analysis was performed using x-ray photoelectron spectroscopy (XPS), both electron (AES) and x-ray-induced (XAES) Auger electron spectroscopy, and secondary electron emission yield measurement (SEE). The SEE coefficient is a valuable measure of the suitability of materials for accelerator and particle storage ring component use because secondary electron emission from such surfaces leads to deleterious effects such as heating, gas desorption, and electrical breakdown. The experimental system has been described previously [4] but, briefly stated, uses Mg or Al anode unmonochromatized x-ray source radiation and a hemispherical electrostatic energy analyzer with 30 eV pass energy (≈ 1 eV energy resolution).

3. Results

3.1. *Heated and room temperature air-oxidized DSC*

The film discussed in the Introduction, and obtained in (b) above, was surface analyzed with the only unusual features in the spectra being those associated with a layer of oxidized boron, which had apparently segregated to the DSC surface during the heat treatment and was subsequently oxidized upon exposure to air. Although the Al 2p and 2s XPS peaks corresponding to surface Al atoms might not be obvious in a Mg Kα XPS spectrum due to their being hidden under the Cu 3p and 3s features, careful comparison of this region of the DSC spectrum with that of a known alumina-free OFE copper sample showed the two to be identical. Moreover, in an experiment using Al Kα primary radiation to try to detect Al by bringing out the Bremsstrahlung-excited XAES peak around 1387 eV kinetic energy, none was observed. Neither was any Al detected by AES analysis of a wide area of the surface, and only a tiny peak corresponding to Al in the bulk appeared in an energy-dispersive x-ray microanalysis (EDX) spectrum taken from this sample. Thus, all attempts to detect alumina in the surface region proved negative, despite the far larger bulk concentration of alumina over that of boron reported in the material specifications.

It should be noted here that the fact that the alumina in the bulk was not detected is in itself unsurprising, since detection limits for the XPS technique are of the order of 10% of a monolayer for adsorbates or about 10^{14} atoms-cm^{-2} which limit is, by the nature of the technique, raised for atoms dispersed in the bulk. Thus, in the absence of migration and bulk concentration of such atoms on the surface, the one volume percent of alumina specified for the material would not be expected to be apparent. What is significant is that the far lower initial concentration of boron atoms does show up, precisely because these atoms evidently undergo a segregation to the surface that the alumina particles do not.

3.1.1. *Patchy boron layer model*

Boron was detected in (a) and (c) as well, but there was appreciably more XPS B 1s signal in the cases of (b) and (c), because of thermally-enhanced segregation to the surface. The B 1s

signal in (b) after heating but prior to air exposure consisted of a single peak whose position corresponds to that of elemental boron, according to our measurements made on an Ar-ion sputter-cleaned boron metal reference sample. After exposure to air of the DSC, the B 1s envelope was observed (Fig. 1) to comprise at least two peaks, centered at binding energy (BE) positions 187.1 and 191.2 eV (relative to Cu $2p_{3/2}$ at 932.4 eV). The low BE peak is the larger of the two, and is assigned as above to elemental boron. The higher BE peak is believed to correspond to an oxide, but it is not clear whether it is the most common boron oxide, B_2O_3, or a defective suboxide or both; the BE of 191.2 eV has nearly the BE shift (4.1 eV, referenced to elemental boron) reported [5] in the literature for B_2O_3 (4.6 eV). Angular XPS data (Fig. 2) show that this "oxide layer" is closer to the surface than the boron species generating the 187.1 eV peak. Moreover, curve-fitting of the B 1s envelope according to procedures previously described in detail [6] suggests that a third peak around 189 eV is also present, which exhibits a similar but less pronounced angular sensitivity. The position of this peak is close to that assigned below to boron nitride, but no nitrogen was detected in this particular sample. Some authors have discussed boron suboxides like B_2O_2 at surfaces [5]; perhaps there is a range of oxygen-deficient possibilities between B and B_2O_3. Incidentally, room temperature air oxidation of our clean boron metal reference sample yields a B 1s spectrum with the same three-peak structure as sample (b).

Comparison of the B 1s intensity measured from (b) with that obtained from the clean boron reference indicates the total boron surface concentration on this DSC sample to be equivalent only to about a monolayer ($\pm30\%$) of which intensity the oxide peaks jointly comprise about a third. However, since the B 1s spectrum exhibits sensitivity to the photoelectron acceptance angle, either this somehow is an underestimate or represents a patchy layer. A single monolayer containing three different species (elemental boron and two oxides) would be of insufficient thickness to structurally exhibit the takeoff angle variations observed above.

3.1.2. *Uniformly distributed boron layer model*

Another possible model exists at this stage, which is that the boron is dispersed to a depth equal to or greater than that sampled by XPS (about 25 Å or so for boron). The lowest BE peak originates from boron that is furthest subsurface, still dissolved in the (increasingly oxygen-free) bulk copper, while the other peak comes from submonolayer levels of oxidized boron closer to the region of the absolute surface, which is largely made up of Cu_2O, according to our XPS Cu 2p and XAES data. This model is discounted, however, on the basis of two things. Firstly, there was only one B 1s peak corresponding to elemental boron present before the sample was exposed to the air, which indicates that at least some of this elemental boron was present at the absolute surface, and secondly, there is the observation that, as indicated above, the bulk of the surface region appears to be Cu_2O, which we know formed at the same time as the surface boron oxide, since there was no oxygen in the spectra prior to air exposure, and if the bulk of the boron atoms detected were dispersed throughout this layer, rather than existing as islands on the surface, they might be expected to oxidize as well, since the reason they are there is because they are efficient scavengers of oxygen. In the light of this, plus the fact that only one boron species, BN, is observed on the surface of the hydrogen-fired sample (c) let up to nitrogen (Section 3.2.), it is assumed that the likeliest model for the surface is one involving the formation of islands or patches of boron metal at the surface during heating of the alloy.

Much more oxygen is present than can be accounted for as B_2O_3, let alone a lower oxide. Therefore it is proposed that the bulk of the "excess" oxygen signal (about 75% of the measured O 1s intensity) over and above that associated with the oxide component of the B 1s spectrum comes purely from a thin layer of copper oxide above bulk copper, which the boron we detect sits in islands upon. The XPS O 1s BE value (530.4 eV) is in agreement with this assignment, and the Cu 2p peak profile together with the Cu LMM XAES peaks support the assignment of Cu_2O as the dominant surface species (although there is some evidence for Cu^0 also, from the XAES data, indicating that the Cu_2O layer is thin). Notwithstanding the latter, the XPS sensitivity-corrected Cu:O intensity ratio came

out to be close to 2:1. Surface carbon levels in the cases of (b) and (c) represent two and one monolayers, respectively, and the position and profile of the C 1s peaks suggests most of this signal is due to graphitic carbon at the surface, so that only a very small proportion of it might account for any more of the O 1s intensity.

3.2. H_2-fired DSC

On the H_2-fired sample, (c), which also had a white film, the B 1s spectrum consists essentially of a single peak at 189.7 eV, fairly confidently assigned to BN according to our measurement on a clean BN reference sample, as well as the fact that not only is nitrogen detected, as a single peak at 397.3 eV [although N is not detected in the cases of (a) or (b)], but the sensitivity-corrected B:N intensity ratio is very close to 1:1. The level of oxygen is significantly lower in (c) than in (b), and the boron concentration, measured relative to an "infinitely thick" boron nitride disc, indicated a BN concentration equivalent to about two atomic monolayers (ca. 4.5 Å). Note that this probably represents a very similar concentration of boron atoms-cm^{-2} of surface as was the case for the non-H_2-fired (b) sample. The co-segregation of boron and nitrogen to form a surface layer of BN has been reported [7] a number of times in the past, over a range of metal surfaces, however, the fact that nitrogen was detected in (c) but not in either (a) or (b) coupled with the fact that (c) is known to have been let up to an atmosphere of nitrogen gas while still warm following its treatment in the furnace, leads more towards the conclusion that the BN was formed during this exposure of the sample to nitrogen and not during the brazing operation.

3.3. Optical examination

At this point, if the white film observed on the surface of (b) is not due to alumina or BN, and cannot be convincingly explained by such a low concentration of boron atoms, the question arises as to what its real origin might be. In order to pursue this question, high magnification optical micrographs were obtained for each of the three samples (Figs. 3-5), and these showed that the surfaces of both (b) and (c), which received exposure to high temperatures, were greatly roughened, particularly when compared to the surface of

unannealed DSC. It has been reported [8] that Glidcop AL-15 samples heated to brazing temperatures exhibit grain coarsening caused by recrystallization. It is therefore concluded that the whitish sheen observed is in large measure due simply to scatter of light at the rough surface of the sample, rather than the presence of any opaque film. It should also be noted that it is possible that such roughness of the surface could, in addition, lead to an underestimation of the real concentration of boron present, due to shadowing effects.

3.4. *SEE results*

For the sake of completeness, we include the SEE yield measurements (Fig. 6) on the DSC surfaces under condition (b) as well as a typical treatment condition used in accelerator structures, i.e., degassing at 250°C to remove water vapor and hydrocarbons. We note that the SEE coefficient has a nominal value of 1.6 whether the surface has been up to brazing temperatures or not, as long as a vacuum bakeout at 250°C takes place after air exposure. Because the SEE yield of oxides is high, it is not surprising the the yield under condition (b) is high. The sharp reduction in yield after bakeout is, however. Disordered adsorbed layers of water vapor and hydrocarbons do substantially increase yields and these are effectively removed by bakeout, but rarely so dramatically. Perhaps, the B_2O_3 surface sorbs a thicker layer than other surfaces.

4. Conclusion

In conclusion, upon heating of the DSC, there occurs a segregation to the surface of some of the residual boron in the sample, forming a thin, patchy layer probably consisting of defective B_2O_3 on top of elemental boron, and accompanied by extensive surface roughening. As indicated above, it has been noted that this type of copper, when used in a brazed construction, suffers from poor wetting performance. It is possible, in the light of the results reported above, that it may be segregation of boron to the solid/gas interface during the brazing process which interferes with the wetting of the DSC. The manufacturer (3) does point out that non-gold-based braze alloys readily diffuse down the grain boundaries of Glidcop DSC but that this problem is minimized with gold alloys. Further experiments on this point are in progress.

Acknowledgments

References

1. K. G. BOUCHARD, *J. Vac Sci. Technol.* **7** (1970) 358.

2. Data sheet, 1988 (SCM Metal Products, Inc., Cleveland, OH 44106, USA).

3. SCM Metal Products, Inc.

4. E. L. GARWIN, F. K. KING, R. E. KIRBY and O. AITA, *J. Appl. Phys.* **61** (1987) 1145.

5. J. KISS, K. REVESZ and F. SOLYMOSI, *Appl. Surface Sci.* **37** (1989) 95.

6. A. R. NYAIESH, E. L. GARWIN, F. K. KING and R. E. KIRBY, *J. Vac. Sci. Technol.* **A4** (1986) 2356.

7. R. H. STULEN and R. BASTASZ, *J. Vac. Sci. Technol.* **16** (1979) 940 and references therein.

8. J. J. STEPHENS, J. A. ROMERO and C. R. HILLS, *Microstructural Science* **16** (1987) 245.

Figure captions

Fig. 1.   DSC XPS B 1s core levels. Heated to 1000°C in vacuum, followed by air exposure. Takeoff angle, relative to DSC surface, $\theta = 75°$. Peak 1, boron metal; peak 2, boron suboxide; peak 3, probably B_2O_3.

Fig. 2.   DSC XPS B 1s core levels. Same as Figure 1, except takeoff angle $\theta = 15°$.

Fig. 3.   DSC, as polished and cleaned for UHV. Shallow isolated pits are typical of this material. Sample condition (a).

Fig. 4.   DSC, heated to 1000°C in UHV, cooled to room temperature and followed by air exposure. Sample condition (b).

Fig. 5.   DSC, heated to 1025°C in H_2 furnace, followed by cooldown with N_2 purge. Sample condition (c).

Fig. 6.   Total secondary electron emission yield of DSC. Yield $= I_{SECONDARY}/I_{PRIMARY}$. Legend: (A) as inserted, condition "a"; (B) heat to 250°C for 6 hours; (C) follow with heat to 1000°C for several minutes, cool and then up to air; (D) follow again with heat to 250°C for 2 hours in vacuum.
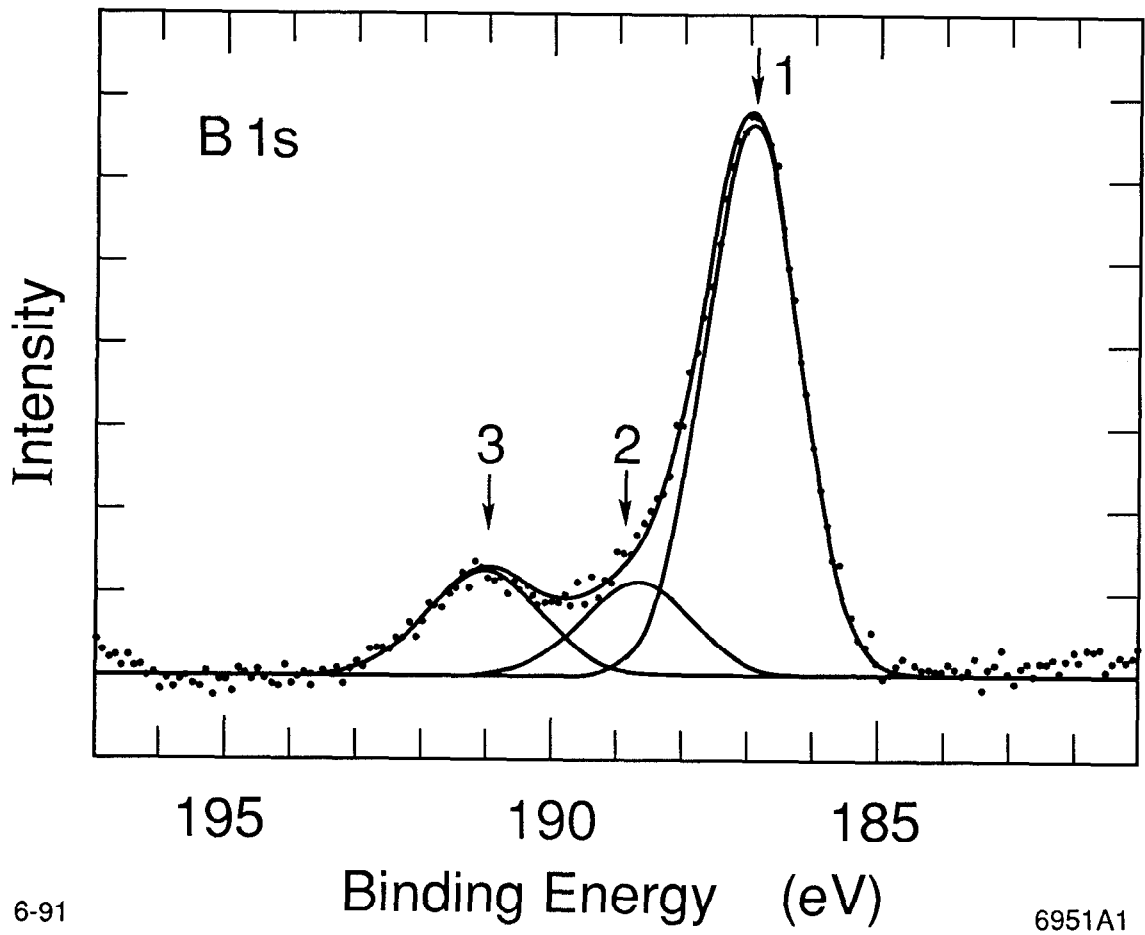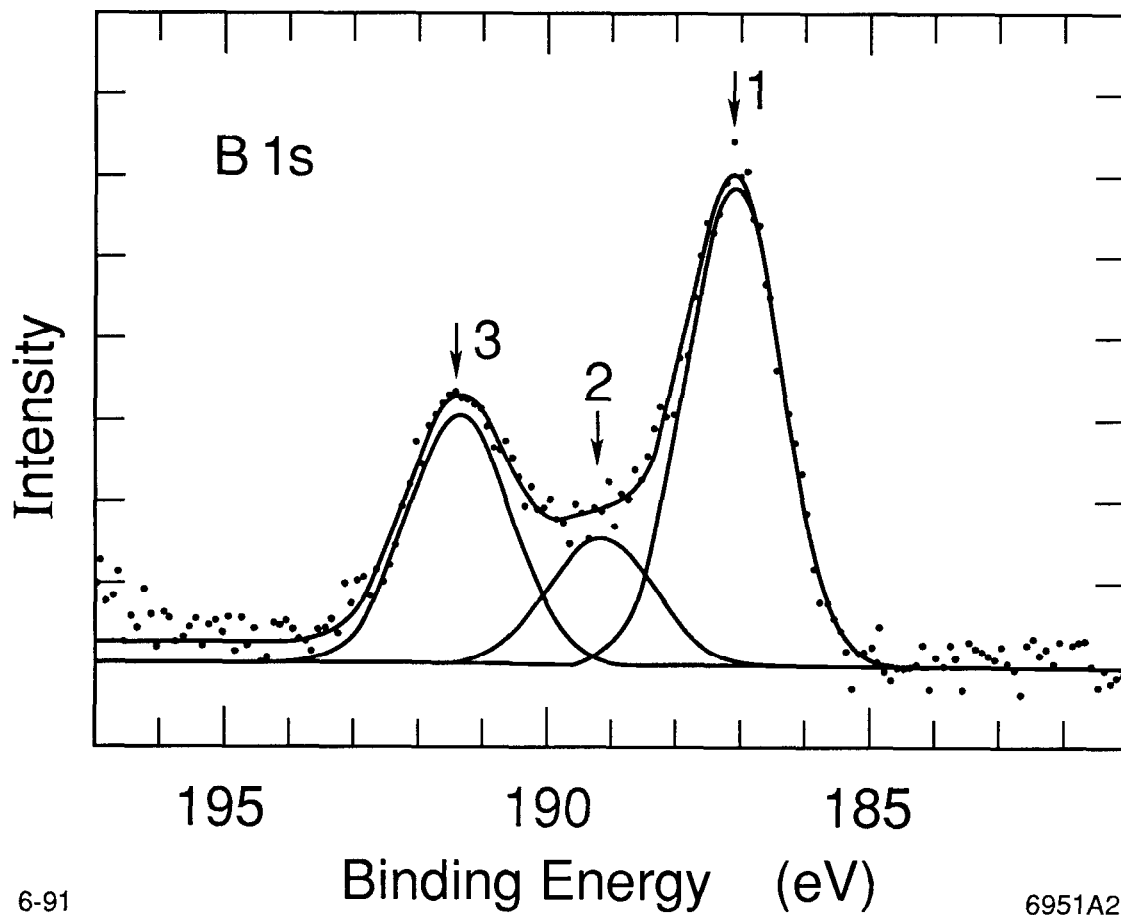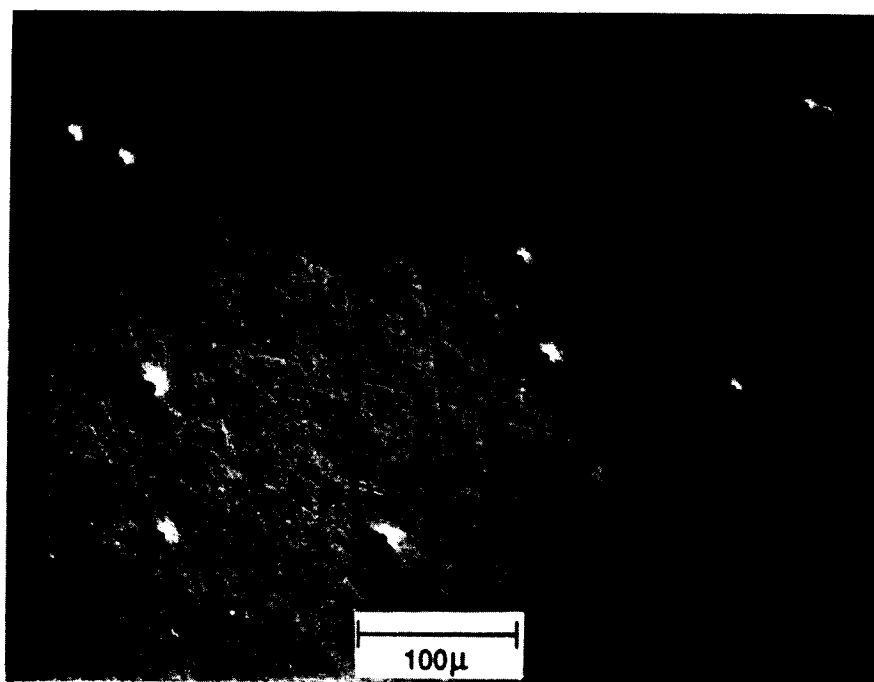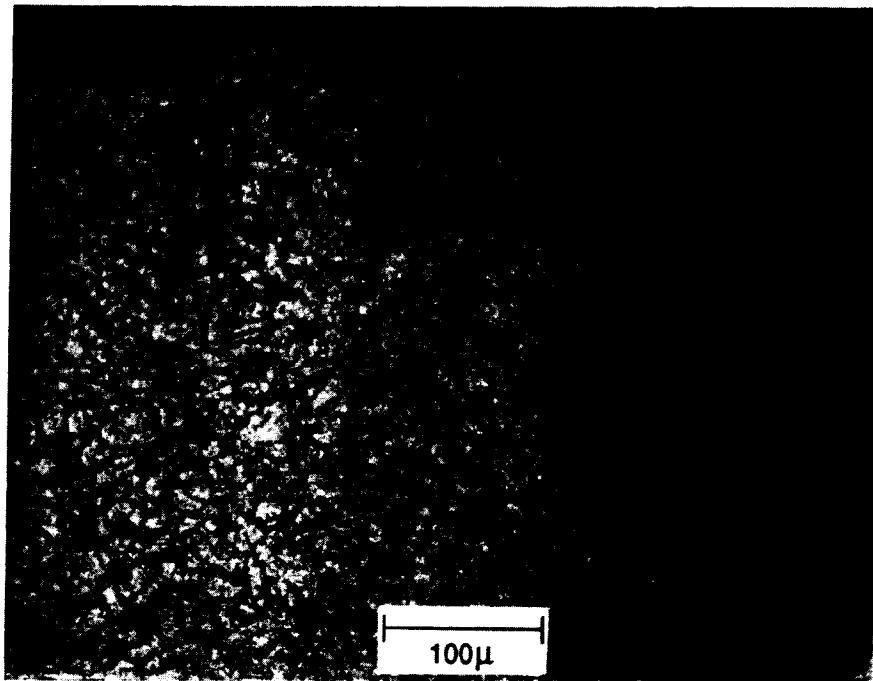
B 1s

1

3   2

Intensity

Binding Energy   (eV)

195   190   185

6-91   6951A1

Fig. 1

B 1s

Intensity

Binding Energy (eV)

6-91

6951A2

Fig. 2

6-91
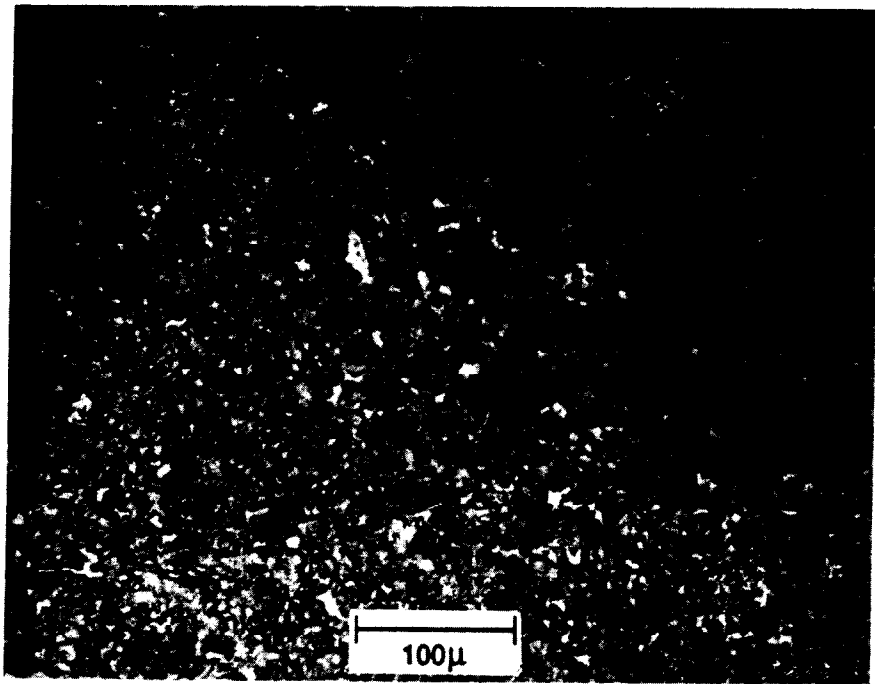
100μ

6951A3

Fig. 3

6-91

100µ

6951A4

Fig. 4

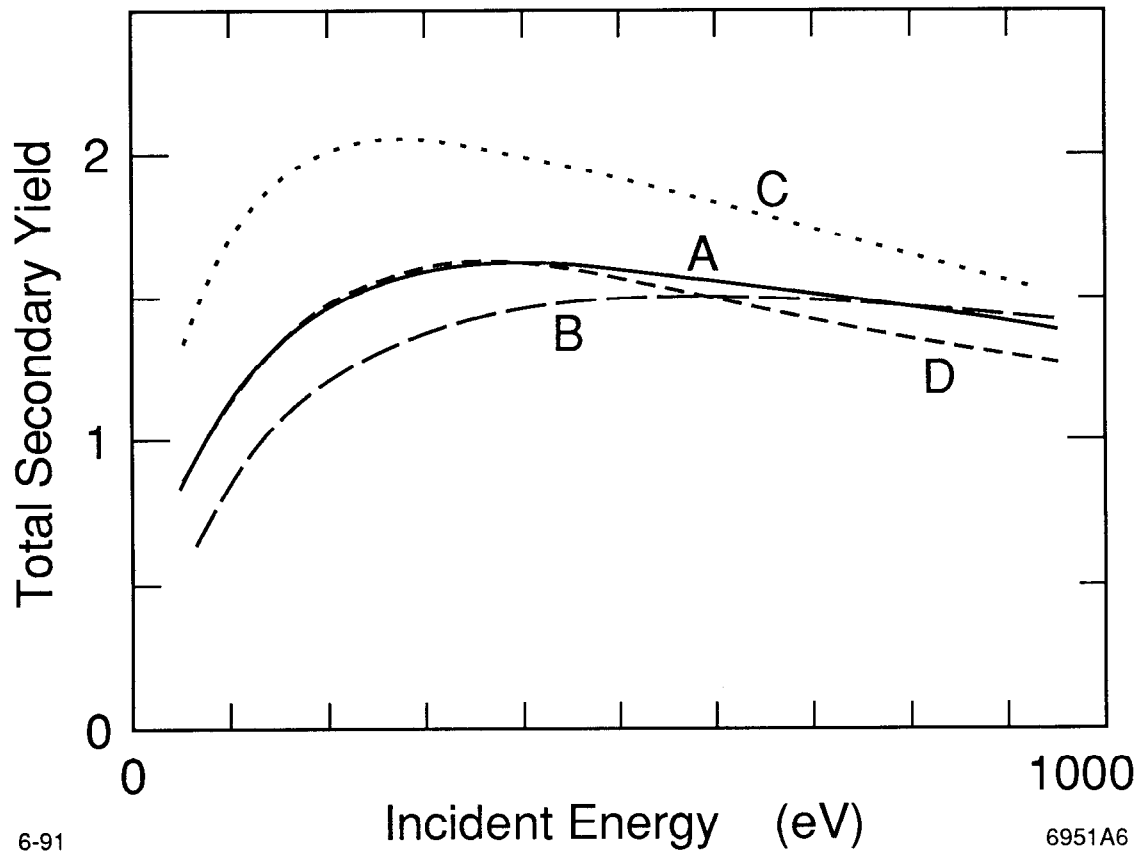6-91   6951A5

Fig. 5

Fig. 6

6-91

6951A6